Numerical approach to the Schrödinger equation in momentum space

William A. Karr, Christopher R. Jamell, and Yogesh N. Joglekar*

Department of Physics, Indiana University Purdue University Indianapolis (IUPUI), Indianapolis, Indiana 46202, USA

Abstract

The treatment of the time-independent Schrödinger equation in real space is an indispensable part of introductory quantum mechanics. In contrast, the Schrödinger equation in momentum space is an integral equation that is not readily amenable to an analytical solution, and is rarely taught. We present a numerical approach to the Schrödinger equation in momentum space. After a suitable discretization process, we obtain the Hamiltonian matrix and diagonalize it numerically. By considering a few examples, we show that this approach is ideal for exploring bound states in a localized potential, and complements the traditional (analytical or numerical) treatment of the Schrödinger equation in real space.

I. INTRODUCTION

The treatment of the time-independent Schrödinger equation for a non-relativistic particle of mass m is a prime element of quantum mechanics courses.[1,2] The treatment of this second-order differential equation introduces students to the effect of boundary conditions on quantization[1] and to the Sturm-Liouville problem.[3,4] For only a few potentials $V(x)$ can the Schrödinger equation

$$-\frac{\hbar^2}{2m}\frac{d^2}{dx^2}\psi_\alpha(x) + V(x)\psi_\alpha(x) = E_\alpha\psi_\alpha(x) \tag{1}$$

be solved analytically, and the eigenvalue spectrum E_α and the complete set of orthonormal eigenfunctions $\psi_\alpha(x)$ be obtained. Introductory texts typically include a quantum well or step, a harmonic oscillator, a delta function potential, and various combinations.[1] The number of analytically solvable potentials is even smaller in higher dimensions. Notable exceptions are those with a central potential where rotational invariance allows us to obtain a second-order differential equation for the radial wavefunction in an effective potential that takes into account the centripetal barrier.[1,2] Although such an equation is not, in general, analytically solvable, it is a significant improvement over the second-order partial differential equation.

To explore the bound states in an arbitrary potential $V(x)$, we can use the Wentzel-Kramers-Brillouin (WKB) approximation[2] which provides a semiclassical picture of quantized energy eigenvalues. Another approach is to discretize Eq. (1) and obtain the matrix equation

$$\sum_{j=-N}^{N}\left[-\frac{\hbar^2}{2m}D_{ij} + V(x_i)\delta_{ij}\right]\psi_\alpha(x_j) = \sum_{j=-N}^{N} H_{ij}\psi_\alpha(x_j) = E_\alpha\psi_\alpha(x_i) \tag{2}$$

where $x_j = j\Delta x$, Δx is the spacing between adjacent points along the discretized x-axis, and $N\Delta x = X_c$ denotes the spatial cutoff chosen such that $X_c \gg a$ where a is the characteristic length scale of the potential $V(x)$. The tridiagonal second-derivative matrix has entries $D_{ij} = \left[\delta_{i,j-1} - 2\delta_{ij} + \delta_{i,j+1}\right]/(\Delta x)^2$. In principle, as $X_c \to \infty$ and $\Delta x \to 0$, the eigenvalues and eigenvectors of the $(2N+1)\times(2N+1)$ matrix H_{ij} approach the spectrum of the original continuum problem. However, due to the diverging prefactor $(\Delta x)^{-2}$ and the error in the matrix D_{ij} at the end-points $\pm X_c$, the matrix diagonalization approach does not lead to stable continuum results. Instead, the Numerov method has to be used to numerically

obtain the eigenvalues and eigenfunctions.[5,6] Another approach is to use the eigenfunction expansion method,[7] which results in a matrix equation for the expansion coefficients.[8]

In this paper we show that the stability and convergence issues[5] are circumvented by the Schrödinger equation in momentum space. In Sec. II we review the equation and the corresponding discretized-matrix eigenvalue problem. This method is ideal for localized potentials with a finite Fourier transform. We present the bound-state spectra for a few well-known potentials and compare them with analytical results whenever possible. In Sec. III we discuss the generalization of our approach to the Schrödinger equation in higher dimensions.[6] We conclude in Sec. IV with a discussion and suggested problems. The method presented here is complementary to the standard differential-equation approach, can be explored in introductory quantum mechanics courses, and is accessible to junior or senior undergraduate students familiar with Matlab, Maple, Mathematica, or LAPACK.

II. SCHRÖDINGER EQUATION IN MOMENTUM SPACE

We start with the Fourier transform of the one-dimensional Schödinger equation, Eq. (1),

$$\epsilon_p \psi_\alpha(p) + \int_{-\infty}^{\infty} \frac{dp'}{(2\pi\hbar)} V(p-p')\psi_\alpha(p') = E_\alpha \psi_\alpha(p). \tag{3}$$

Here $\psi_\alpha(p)$ is the momentum-space wavefunction, which represents the probability amplitude for the particle to have momentum p, $\epsilon_p = p^2/2m$ is the (non-relativistic) kinetic energy of the particle, and $V(q)$ is the Fourier transform of the external potential $V(x)$. We use the same symbol for the eigenvector $|\psi_\alpha\rangle$ and the potential energy operator $\hat{V}$ in both real and momentum space; the fact that $\psi_\alpha(x)$ and $\psi_\alpha(p)$ are different functions is understood.[9,10] The integral equation (3) has been used to study the scattering problem[10,11] and the bound state in a δ-function potential.[12]

To convert Eq. (3) into a form suitable for numerical exploration, we use a_0 to denote the length-scale, define the momentum scale by $\hbar/a_0$, and use $E_0 = \hbar^2/2ma_0^2$ as the unit of energy. Because a_0 is arbitrary in the continuum limit, the spectrum with a potential characterized by depth V_0 and range a, $V(x) = V_0 f(x/a)$, is determined by the dimensionless parameter $V_0/E_a = V_0/(\hbar^2/2ma^2)$. For the numerical calculations it will be useful to choose $V_0/E_0 = 1$ and vary a/a_0 to access various values of V_0/E_a. In terms of the dimensionless

variables Eq. (3) leads to a matrix equation after discretization:

$$\left[u_n^2\delta_{mn} + \tilde{V}_{mn}\right]\psi_\alpha(u_n) = H_{mn}\psi_\alpha(u_n) = \tilde{E}_\alpha\psi_\alpha(u_m), \tag{4}$$

where a sum over the repeated index n is understood. Here $u_n = n\Delta u = n\Delta p a_0/\hbar = p_n a_0/\hbar$ is the dimensionless momentum, Δu is the spacing between adjacent points along the u-axis, $\tilde{E}_\alpha = E_\alpha/E_0$ is the dimensionless eigenvalue, and $\tilde{V}_{mn} = V(p_m - p_n)\Delta u/(2\pi E_0 a_0)$ is the dimensionless potential along with the discrete measure $\Delta u/(2\pi)$. Thus, the integral Schrödinger equation (3) has been recast as a matrix eigenvalue problem, Eq. (4). The eigenvalues and eigenvectors of the dimensionless Hamiltonian matrix H_{mn} are obtained using standard software packages. The results presented here were obtained by using Matlab and were verified by using LAPACK. This discretization process involves some computational subtleties that we discuss in the following, but provides an excellent way to study bound states in potentials that are localized in real space.

The size of the Hamiltonian matrix H_{mn} is determined by the dimensionless ultraviolet momentum cutoff $U_c = P_c a_0/\hbar$, where P_c is upper limit of the integration range in Eq. (3), and the dimensionless spacing Δu. Note that $2\pi a_0/\Delta u$ and $2\pi a_0/U_c$ impose the upper and lower limit respectively on the real-space size of the bound-state wavefunction. Thus, they need to be chosen for a given potential so as to obtain results that are valid in the continuum limit, $U_c \to \infty$ and $\Delta u \to 0$. If the external potential $V(x)$ is even, the Hamiltonian H_{mn} is real. Therefore, the eigenfunctions $\psi_\alpha(p)$ have a definite parity and are real.[2] In this case it is sufficient to restrict ourselves to positive momenta $m, n \geq 0$.

To demonstrate these considerations, we start with a quantum well with depth V_0 and width a centered at the origin, $V(x) = -V_0\theta(a-2|x|) = V(-x)$ where $\theta(x)$ is the Heavy-side function.[3,4] In this case the real Hamiltonian matrix is given by

$$H_{mn} = u_n^2\delta_{mn} - \frac{\Delta u}{2\pi}\frac{2aV_0}{a_0E_0}\frac{\sin\left[(u_n - u_m)a/a_0\right]}{\left[(u_n - u_m)a/a_0\right]} = H_{nm}. \tag{5}$$

The factor of 2 in the potential matrix elements arises from the restriction $m, n \geq 0$. The one-dimensional δ-function potential, $V(x) = -\lambda_1\delta(x)$, is obtained as a limiting case when $a \to 0$, $V_0 \to \infty$ with $aV_0 = \lambda_1$. In this limit for an attractive potential, $\lambda_1 > 0$, the system has one exponentially bound state $\psi_b(x) = \sqrt{\kappa}\exp(-\kappa|x|)$ with size $\kappa^{-1} = \hbar^2/m\lambda_1$ and energy[1,2] $E_b = -m\lambda_1^2/2\hbar^2$.

We obtain the eigenvalues and eigenvectors of the matrix H_{mn} for $0 \leq |\lambda_1/E_0a_0| \leq 1$ with two different values of $\Delta u = \{0.01, 0.005\}$ and two different cutoffs $U_c = \{10, 20\}$. The

corresponding matrix dimension $N = U_c/\Delta u$ in these four cases varies from 1000×1000 to 4000×4000. We find that the energy spectrum has one negative eigenvalue and the positive eigenvalues form a quadratic band representative of a free particle. (The positive-energy unbounded states are not accessible via the Numerov method.[5]) Figure 1(a) shows that the bound-state energy $E_b(\lambda_1)$ matches the analytical result. Figure 1(b) shows a typical momentum-space wavefunction for the bound-state $\psi_b(p)$ and a state with positive energy. As expected, we see that the bound-state wavefunction, $\psi_b(p) = 2(\hbar\kappa)^{3/2}/(p^2 + \hbar^2\kappa^2)$, is broad, whereas the positive-energy wavefunction is sharply peaked near a single momentum value. We check that the bound-state results are independent of U_c and Δu. (The smallest momentum cutoff is chosen such that the contribution from momenta $p > P_c = U_c\hbar/a_0$ to the bound-state wavefunction is negligible.) Increasing U_c affects the eigenvalues and eigenvectors near the highest energy $E_c/E_0 = U_c^2$, whereas reducing Δu sharpens the momentum-space eigenfunctions at positive energies. Thus, this numerical approach is particularly suited to study bound states, and may not handle the unbounded positive-energy states equally well.

Next, we consider the problem of a deep quantum well $V_0/E_a \gg 1$. We diagonalize the matrix H_{mn}, Eq. (5), with $V_0/E_0 = 1$, $U_c = 300$, $\Delta u = 0.1$, and $a/a_0 = \{20, 25\}$. Figure 2 shows that the numerically obtained spectrum of the bound-state energies measured from the bottom of the quantum well is quadratic, $E_n = n^2\pi^2\mathcal{E}$. This dependence is expected because for an infinite quantum well of size a the eigenvalues are given by $E_n = n^2\pi^2 E_a$. The prefactor $\mathcal{E}(U_c, \Delta_u, V_0) \neq E_a$, and a systematic exploration with increasing U_c and a, and decreasing Δu shows that this discrepancy is due only to the discretization. We next consider an attractive Gaussian potential $V_1(x) = -V_0 \exp(-x^2/2a^2)$. In this case a closed-form solution for the eigenvalues and eigenfunctions is unknown. The dimensionless Hamiltonian becomes

$$H^{(1)}_{mn} = u_n^2\delta_{mn} - \frac{\Delta u}{\sqrt{2\pi}}\frac{2V_0 a}{E_0 a_0}\exp\left[-\frac{(u_m - u_n)^2 a^2}{2a_0^2}\right] = H^{(1)}_{nm}. \tag{6}$$

Figure 3 shows the a-dependence of the magnitude of the ground-state energy $E_b < 0$ obtained by using $V_0/E_0 = 1$, $\Delta u = 0.01$, and $U_c = 30$. The inset shows the ground state momentum-space wavefunction $\psi_G(p)$ for $a/a_0 = \{0.1, 0.5\}$. As a/a_0 increases, the effective value of V_0/E_a increases. Thus, the ground state becomes more localized in real-space, and the spread of the wavefunction in momentum-space increases.

We emphasize that the bound-state eigenvalues and eigenfunctions obtained from the diagonalization of the discrete matrix H_{mn} should be essentially independent of the cutoff $U_c \gg 1$ and the spacing $\Delta u \ll 1$, to verify that they are valid in the continuum limit $U_c \to \infty$, $\Delta u \to 0$. Note that even in the limit $\Delta u \to 0$, a finite momentum-cutoff P_c leads to a real-space potential that is not the same as the original one:

$$V_c(x) = \int_{-P_c}^{P_c} \frac{dp}{2\pi\hbar} V(p) e^{ipx/\hbar} \neq V(x). \tag{7}$$

Thus the discretization parameters need to be so chosen that the difference between $V_c(x)$ and $V(x)$ is negligible. Two typical indicators that the continuum limit has not been reached are that some eigenvalues are lower than the depth of the potential well, $E_\alpha < -V_0$, and the ground-state momentum-space wavefunction is linear, instead of quadratic, near $p = 0$. In one dimension we can choose the ground state wavefunction $\psi_G(x)$ to be positive,[1,2] so that, for an even potential the momentum-space wavefunction is parabolic at the origin, $\psi_G(p) - \psi_G(p = 0) \propto -p^2$. Therefore, a linearly varying $\psi_G(p)$ is a clear indication that the bound-state eigenvalues and eigenfunctions do not represent continuum results. In the following we show that the verification of the continuum limit is more subtle in two dimensions and requires a careful treatment.

III. NUMERICAL APPROACH IN HIGHER DIMENSIONS

For a particle in two or more dimensions, a naive discretization of the integral Schrödinger equation in Cartesian co-ordinate implies that the Hamiltonian matrix has a size $\sim N^D \times N^D$ where $N = U_c/\Delta u$ is the number of discrete points along a single axis and D is the dimension. Thus, even in two dimensions, the parameters used in Sec. II result in $10^6 \times 10^6$ or larger matrices that are impossible to treat numerically. For a central potential in two dimensions, the rotational invariance of the Hamiltonian implies that the angular momentum is a good quantum number and the eigenfunctions can be labeled by an integer angular momentum label ℓ, $\psi_\alpha(\mathbf{p}) = \psi_{\alpha\ell}(p) \exp(i\ell\theta_p)$, where $\mathbf{p} = (p, \theta_p)$ is the two-dimensional momentum.[1,2,10] The Schrödinger equation for a given value of ℓ becomes[6]

$$\frac{p^2}{2m}\psi_{\alpha l}(p) + \int \frac{p' dp' d\theta_{p'}}{(2\pi\hbar)^2} V(p, p'; \theta_p - \theta_{p'}) e^{-i\ell(\theta_p - \theta_{p'})} \psi_{\alpha\ell}(p') = E_{\alpha\ell}\psi_{\alpha\ell}(p) \tag{8}$$

where $V(p, p'; \theta_p - \theta_{p'}) = V(|\mathbf{p} - \mathbf{p}'|)$ is the momentum-space potential and depends only on the angle between $\mathbf{p}$ and $\mathbf{p}'$ due to the central nature of the potential. The corresponding

dimensionless Hamiltonian matrix becomes $H_{mn}(\ell) = u_n^2\delta_{mn} + \tilde{V}_{mn}(\ell)$, where the angular-averaged potential matrix is given by

$$\tilde{V}_{mn}(\ell) = \frac{u_n \Delta u}{2\pi E_0 a_0^2} \int_0^{2\pi} \frac{d\theta}{2\pi} V(u_m, u_n; -\theta) e^{i\ell\theta}. \tag{9}$$

Here, $0 \leq u_n \leq U_c$ denotes the magnitude of the dimensionless momentum and the matrix $H_{mn}(\ell)$ has size $\sim N \times N$. Due to the prefactor $u_n \Delta u$ from the two-dimensional area-element in polar co-ordinates, the Hamiltonian obeys $H_{nm}(\ell) = (u_m/u_n) H^*_{mn}(\ell)$. Thus, the discretized Hamiltonian matrix is not Hermitian with respect to transpose of the matrix plus complex conjugation. It is Hermitian with respect to the inner product defined via the two-dimensional measure. We will focus on $\ell = 0$ case because for a time-reversal invariant Hamiltonian, the ground state has zero angular momentum.[2,10]

As an illustration, we consider an attractive δ-function potential in two dimensions, $V(\mathbf{r}) = -\lambda_2 \delta^2(\mathbf{r})$. Although a trivial extension of the one-dimensional problem, it is rarely discussed[13] in introductory courses, perhaps because the bound-state real-space wavefunction is logarithmically divergent[14] in the vicinity of the δ-function. The bound-state energy $E_b(\lambda_2, U_c)$ depends on the ultraviolet cutoff U_c and has a non-analytic dependence on the strength of the potential, $E_b/E_0 = -U_c^2 \exp(-4\pi E_0 a_0^2/\lambda_2)$.[13,15] The momentum-space Schrödinger equation in this case is analytically tractable and provides a good test.[15] Because the Fourier transform of this potential is a constant, the Hamiltonian matrix becomes

$$H_{mn}(\ell) = u_n^2 \delta_{mn} - \frac{u_n \Delta u}{2\pi} \frac{\lambda_2}{E_0 a_0^2} \delta_{\ell 0} = \frac{u_n}{u_m} H_{nm}(\ell). \tag{10}$$

The δ-function potential affects only $\ell = 0$ sector of the Hilbert space because wavefunctions with $\ell \neq 0$ vanish at the position of the δ-function due to the centripetal barrier. We verify that there is a single bound state for an attractive potential ($\lambda_2 > 0$) and none for a repulsive potential ($\lambda_2 < 0$). Figure 4 shows the magnitude of the bound-state energy $E_b(\lambda_2)$ as a function of $4\pi E_0 a_0^2/\lambda_2$ for $2 \leq \lambda_2/E_0 a_0^2 \leq 20$. We use $\Delta u = 0.01$ and two ultraviolet cutoffs $U_c = \{10, 20\}$. At large values of $\lambda_2/E_0 a_0^2 \sim U_c$, the numerical results deviate from the expected straight-line behavior due to discretization. This deviation is systematically suppressed by reducing Δu. Note that for an attractive δ-potential in both one and two dimensions the bound-state wavefunction has the same functional form, $\psi_b(p) \propto 1/(p^2 + \hbar^2\kappa^2)$. However, because the bound-state energy $E_{b2} \propto \exp(-1/\lambda_2)$ in two dimensions[13], in contrast to the bound-state energy $E_{b1} \propto \lambda_1^2$ in one dimension,[1,2] the size of the wavefunction

in momentum-space in two dimensions is much smaller than that in one dimension, $\hbar\kappa_2 = \sqrt{2m|E_{b2}} \ll \hbar\kappa_1 = \sqrt{2m|E_{b1}|}$. We emphasize that the dependence of E_b on the cutoff U_c is a peculiar property of the weakly bound state in the two-dimensional δ-function potential and arises due to the absence of an energy scale in a problem characterized by $(\hbar, m, \lambda_2)$. For a general potential, including the attractive Coulomb interaction $V(r) = -e^2/r$, we numerically obtain multiple bound-states with energies that are independent of the cutoff.[16]

For a central potential it is straightforward to extend this method to higher dimensions. In D-dimensions we represent a vector using hyperspherical co-ordinates, $\mathbf{p} = (p, \phi, \theta_1, \theta_2, \ldots, \theta_{D-2})$ where $\phi \in [0, 2\pi]$ and $\theta_i \in [0, \pi]$.[17] The Hamiltonian is then block-diagonalized into blocks with different angular momenta. The effective potential in the block (ℓ, ℓ_z) is obtained by performing an integral over angular variables, similar to that in Eq. (9). It is not always possible to analytically carry out this integration. The resulting Hamiltonian matrix satisfies $H_{nm}(\ell, \ell_z) = (u_m/u_n)^{D-1} H^*_{mn}(\ell, \ell_z)$, and the resulting eigenvectors $\psi_\alpha(u_k)$ are orthogonal with respect to the D-dimensional inner product

$$\langle \psi_\alpha | \psi_\beta \rangle = \frac{\Delta u}{2\pi} \sum_{k=0}^{N} \psi^*_\alpha(u_k) \psi_\beta(u_k) u_k^{D-1} = 0 \qquad (\alpha \neq \beta). \tag{11}$$

The exploration of the Hamiltonian matrix $H_{mn}(\ell, \ell_z)$ in $D \geq 2$ dimensions emphasizes two important points. First, by explicit construction, it generates a set of matrices, each element of which appears non-Hermitian and still has a purely real eigenvalue spectrum. Second, it explicitly demonstrates that the notion of orthonormality and Hermiticity are intimately connected to the inner-product used to construct the Hilbert space of wavefunctions.[1]

IV. CONCLUSIONS

We have presented an approach to the real-space Schrödinger equation via the Hamiltonian matrix in momentum-space that is obtained after a suitable discretization.[6] This method does not suffer from the instability associated with discretization of the real-space Schrödinger equation,[5] primarily because the kinetic energy term is diagonal in momentum space and, for most physical potentials, the amplitude $\tilde{V}_{pp'}$ for scattering from p to p' decays for large $|p - p'|$. Therefore, the elements of the matrix H_{mn} near the top-right and bottom-left corners are small.

Our method is best suited for numerically investigating the energies and wavefunctions

of bound states that occur in a localized central potential $V(r)$ with a finite Fourier transform $V(q)$. Many well-known examples with confining potentials where all eigenstates are localized (an infinite quantum well or a simple harmonic oscillator) cannot be studied using our approach because the Fourier transform is ill-defined. However, as we have discussed in Sec. II, it is possible to explore the low-lying eigenstates of such a system by choosing parameters such that $V_0/E_a = V_0/(\hbar^2/2ma^2) \gg 1$. Such a deep well, as far as the low-lying eigenstates are concerned, can be treated as an infinite well.

V. SUGGESTED PROBLEMS

Problem 1. Obtain the bound-state spectra for the potential

$$V_\eta(x) = \begin{cases} -V_0[1 - (2|x|/a)^\eta] & |x| < a/2 \\ = 0 & \text{otherwise,} \end{cases} \tag{12}$$

where $\eta > 0$. Note that $V_\eta(x)$ represents a family of potentials that extrapolate from a linear ($\eta = 1$), a quadratic ($\eta = 2$), to a quantum well ($\eta \to \infty$). Choose $V_0/E_a = V_0/(\hbar^2/2ma^2) \gg 1$. Compare your results to the WKB approximation prediction $E_k = -A_\eta[2k+1]^{2\eta/(2+\eta)}$, where A_η is a constant and the eigenenergies E_k are measured from the bottom of the potential well.

Problem 2. Obtain the analog of Eq. (10) in three dimensions and study the spectrum for a given cutoff U_c. Show that a bound state arises only when $\lambda_3 \geq \lambda_{3c} \sim 1/U_c$, and determine λ_{3c}. Contrast your results with those for a quantum well with depth V_0 and size $\hbar/P_c = a_0/U_c$.

Acknowledgments

W.A.K. was supported by the IUPUI Undergraduate Research Opportunity Program (UROP) through a Summer Fellowship. C.R.J. was supported by the National Science Foundation GAANN Fellowship. We are thankful to an anonymous referee for pointing out

Ref. 6 to us.

---

* Electronic address: yojoglek@iupui.edu

[1] D. J. Griffiths, *Introduction to Quantum Mechanics* (Prentice Hall, Englewood Cliffs, NJ, 2004).

[2] E. Merzbacher, *Quantum Mechanics* (John Wiley & Sons, Hoboken, NJ, 1998).

[3] E. Kreyszig, *Advanced Engineering Mathematics* (John Wiley & Sons, Hoboken, NJ, 2006), pp. 188–193.

[4] P. Dennery and A. Krzywicki, *Mathematics for Physicists* (Dover, Mineola, NY, 1995).

[5] P. C. Chow, "Computer solutions to the Schrödinger equation," Am. J. Phys. **40**, 730–734 (1972).

[6] R. H. Landau, M. José Páez, and C. C. Bordeianu, *A Survey of Computational Physics* (Princeton University Press, Princeton, NJ, 2008).

[7] E. C. Titchmarsh, "Some eigenfunction expansion formulae," Proc. London Math. Soc. **11**, 159–168 (1960) and references therein; C. E. Dean and S. A. Fulling, "Continuum eigenfunction expansions and resonances: A simple model," Am. J. Phys. **50**, 540–544 (1982).

[8] See Chap. 4 in Refs. 3,4.

[9] P. A. M. Dirac, *The Principles of Quantum Mechanics* (Oxford University Press, New York, 1996).

[10] J. J. Sakurai, *Modern Quantum Mechanics* (Addison -Wesley, Reading, MA, 1995).

[11] A. Goldberg, H. M. Schey, and J. L. Schwartz, "One-dimensional scattering in configuration space and momentum space," Am. J. Phys. **36**, 454–455 (1968); S. K. Adhikari, "Quantum scattering in two-dimensions," Am. J. Phys. **54**, 362–367 (1986).

[12] M. Lieber, "Quantum mechanics in momentum space: An illustration," Am. J. Phys. **43**, 486–491 (1975).

[13] L. D. Landau and E. M. Lifshitz, *Quantum Mechanics (Non-Relativistic Theory)* (Butterworth-Heinemann, Burlington, MA, 2005), Sec. 45.

[14] J. Fernando Perez and F. A. B. Coutinho, "Schrödinger equation in two dimensions for a zero-range potential and a uniform magnetic field: An exactly solvable model," Am. J. Phys. **59**, 52–54 (1991).

[15] S. Nyeo, "Regularization methods for delta-function potential in two-dimensional quantum me-

chanics," Am. J. Phys. **68**, 571–575 (2000).

[16] J. W. Huang and A. Kozycki, "Hydrogen atom in two dimensions," Am. J. Phys. **47**, 1005–1006 (1979); X. L. Yang, M. Lieber, and F. T. Chan, "The Runge-Lenz vector for the two-dimensional hydrogen atom," Am. J. Phys. **59**, 231–232 (1991); C. R. Jamell, C.-H. Zhang, and Y. N. Joglekar, "Dilute excitons in a double-layer system: single exciton and mean-field approach," arXiv:0910.2993.

[17] L. E. Blumenson, "A derivation of n-dimensional spherical coordinates," Am. Math. Monthly **67**, 63–66 (1960); E. Demiralp, "Bound states of n-dimensional harmonic oscillator decorated with Dirac delta functions," J. Phys. A **38**, 4783–4793 (2005).

Figure captions

FIG. 1: (color online) (a) Dependence of the magnitude of the bound-state energy $|E_b|$ obtained from the matrix H_{mn}, Eq. (5), on the strength λ_1 of the one-dimensional attractive δ-function potential. The energy is in units of $E_0 = \hbar^2/2ma_0^2$ and λ_1 is in units of $E_0 a_0$. The numerical result (crosses) is in excellent agreement with the analytical result[1,2] $|E_b|/E_0 = \lambda_1^2/4(E_0 a_0)^2$ (dashed line). (b) Typical momentum-space wavefunctions for the bound state (top curve) and a positive-energy state (bottom curve) for $\lambda_1/E_0 a_0 = 0.5$. The momentum p is in units of $a_0/\hbar$ and the wavefunction is in units of $\sqrt{a_0}$. The width of the bound-state wavefunction $\psi_b(p)$ is given by $\hbar\kappa = m\lambda_1/\hbar$. The positive-energy wavefunction is, as expected, sharply localized in momentum space.

FIG. 2: (color online) Eigenenergies E_n of bound states in a deep quantum well $V_0/E_a \gg 1$ obtained from Eq. (5). The bound-state energies E_n are positive because they are measured from the bottom of the well. The energies are in units of $E_a = \hbar^2/2ma^2 = E_0(a_0/a)^2$ instead of the customary unit E_0. The solid and the dashed lines represent results for $V_0/E_a = (a/a_0)^2 = 400$ and 625 respectively. The dotted line shows the analytical result for an infinite quantum well of width a, $E_n = (n\pi)^2 E_a$.

FIG. 3: (color online) Magnitude of the ground-state energy $|E_b|$ for a Gaussian potential $V(x) = -V_0 \exp(-x^2/2a^2)$ as a function of a for a fixed depth $V_0/E_0 = 1$. The energies are in units of E_0, the length is in units of a_0, and the momentum in the inset is in units of $\hbar/a_0$. The inset shows the ground-state momentum-space wavefunction in units of $\sqrt{a_0}$. As a increases, the ground-state wavefunction becomes increasingly localized in real space, and is reflected in the broadening of the momentum-space wavefunction.

FIG. 4: (color online) Dependence of $|E_b|$ on the strength λ_2 of the attractive two-dimensional δ-function potential for ultraviolet momentum cutoffs $U_c = 10$ (squares) and $U_c = 20$ (circles). The energy is in units of E_0 and λ_2 is in units of $E_0 a_0^2$; $\Delta u = 0.01$ and $2 \leq \lambda_2/E_0 a_0^2 \leq 20$. The solid lines represent the analytical result, $\ln(|E_b|/E_0) = -4\pi E_0 a_0^2/\lambda_2 + \ln(U_c^2)$ for $U_c = 10$ (bottom curve) and $U_c = 20$ (top curve). The corresponding y-intercepts are $\ln(10^2) \approx 4.6$ and $\ln(20^2) \approx 6$. The discrepancy between the numerical and analytical results for large $\lambda_2/E_0 a_0^2 \sim U_c$ is decreased when Δu is reduced.

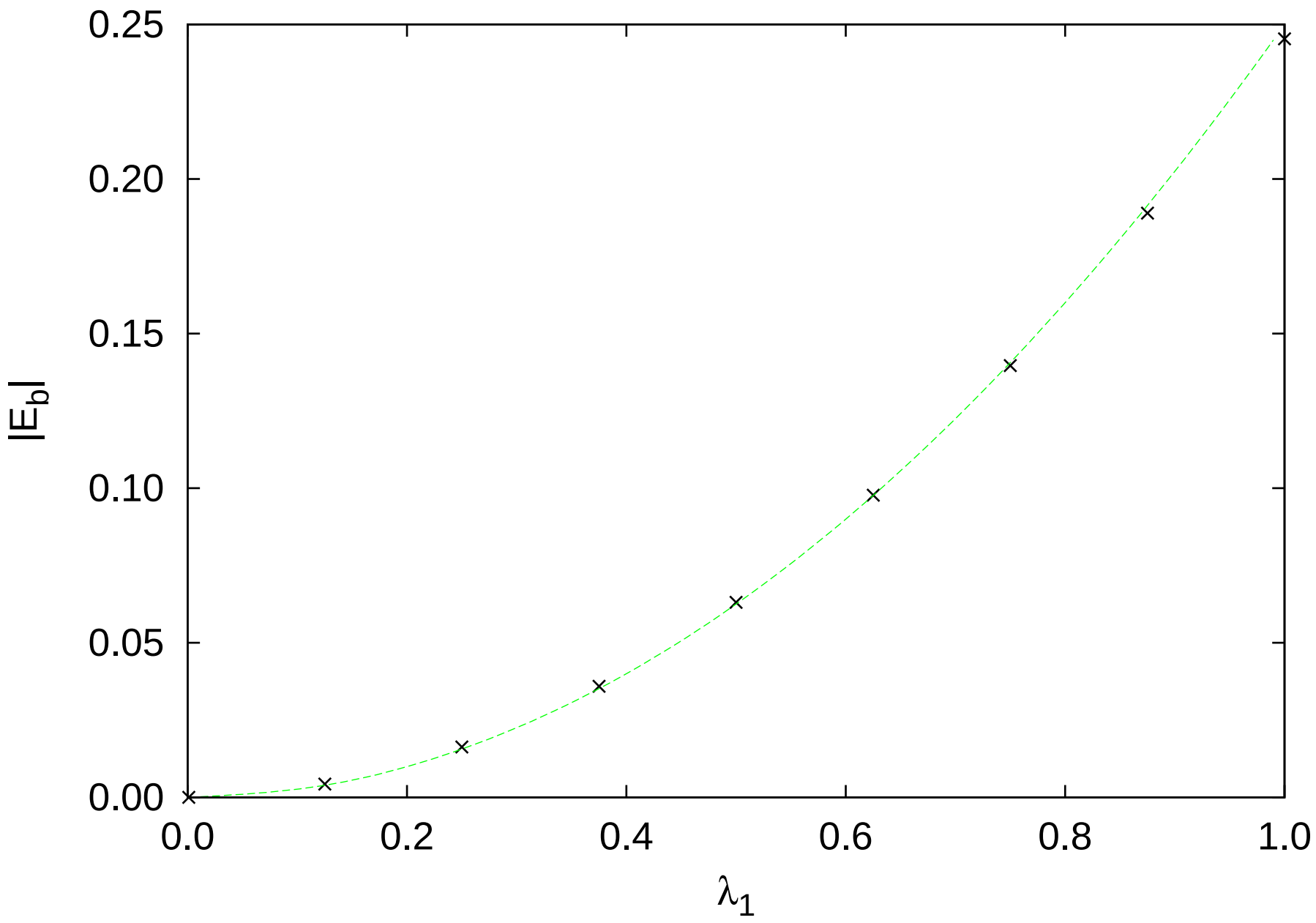
0.25
0.20
0.15
0.10
0.05
0.00
|E_b|
0.0
0.2
0.4
0.6
0.8
1.0
λ_1

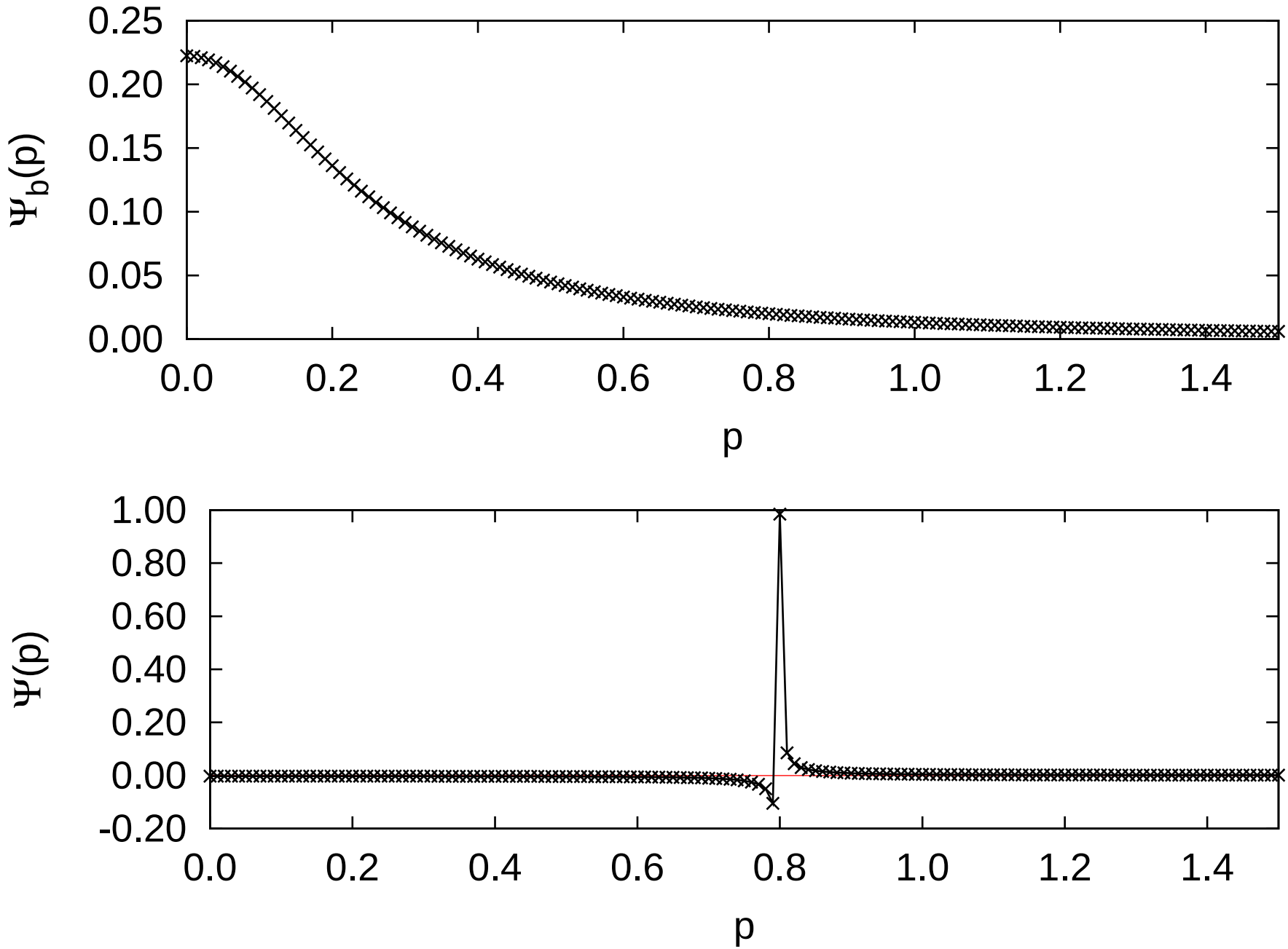
0.25
0.20
0.15
0.10
0.05
0.00
$\Psi_b(p)$
0.0
0.2
0.4
0.6
0.8
1.0
1.2
1.4
p
1.00
0.80
0.60
0.40
0.20
0.00
-0.20
$\Psi(p)$
0.0
0.2
0.4
0.6
0.8
1.0
1.2
1.4
p

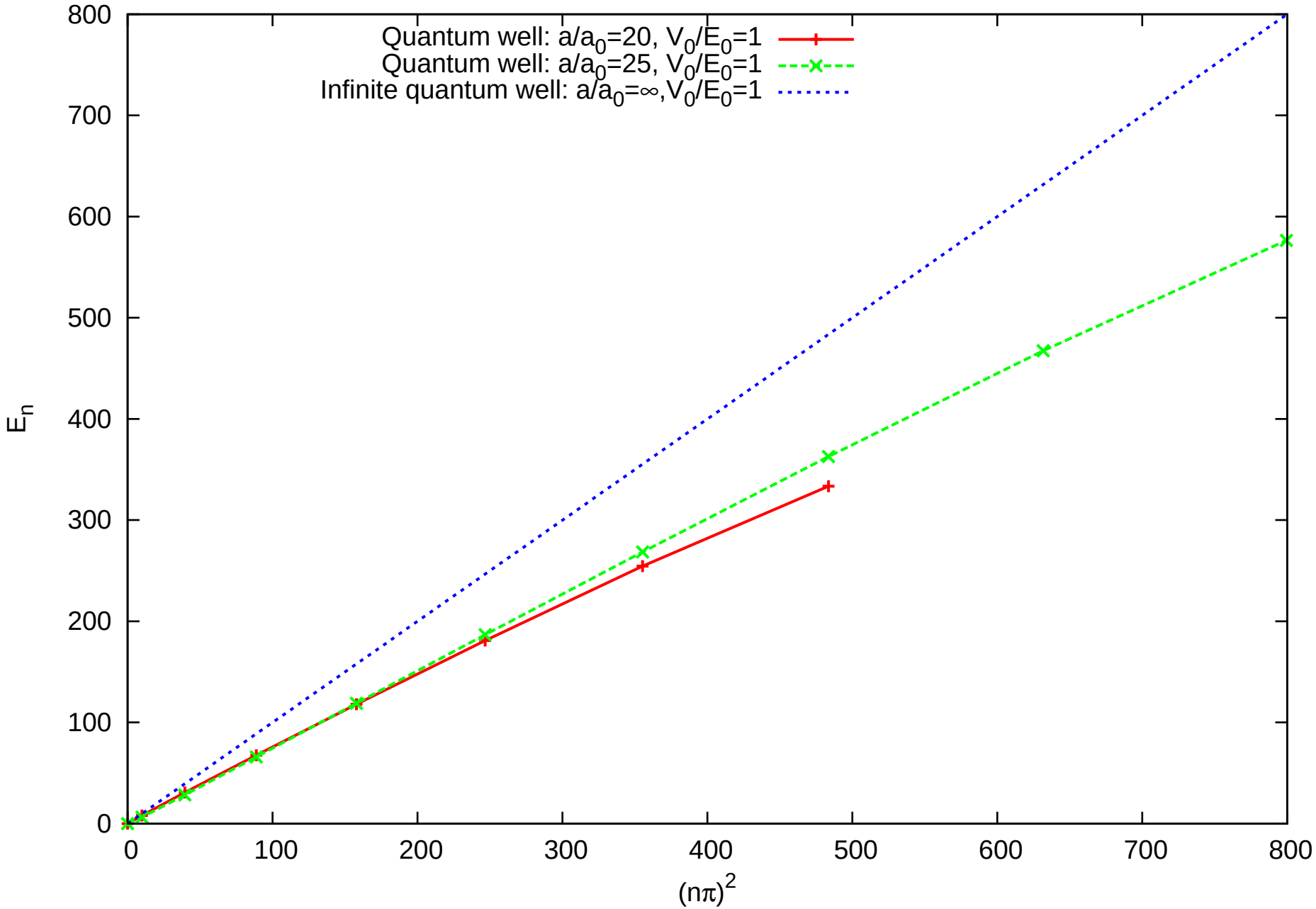
Quantum well: a/a0=20, V0/E0=1
Quantum well: a/a0=25, V0/E0=1
Infinite quantum well: a/a0=∞,V0/E0=1
En
(nπ)2
0
100
200
300
400
500
600
700
800

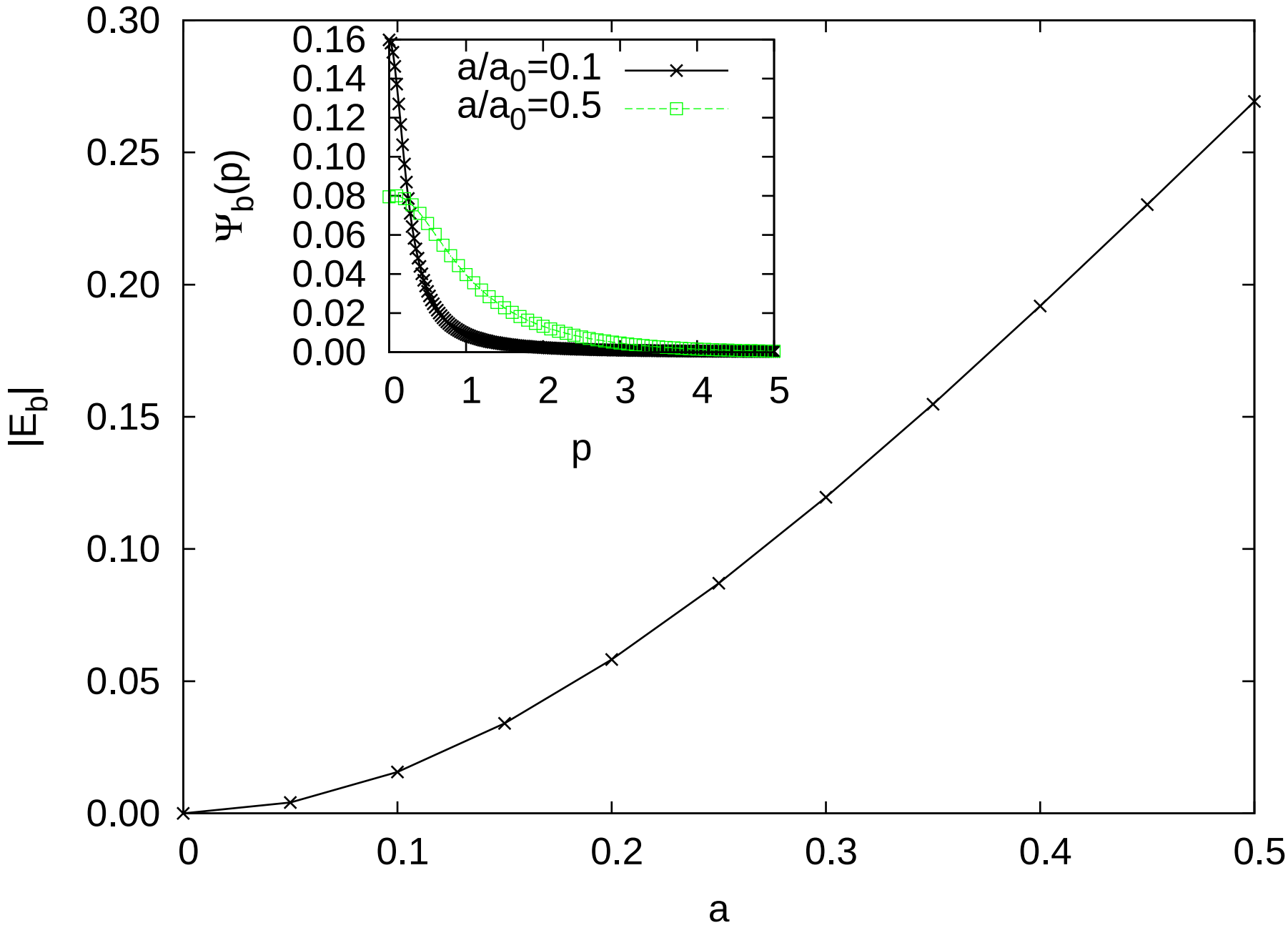
0.30
0.25
0.20
0.15
0.10
0.05
0.00
|E_b|
0
0.1
0.2
0.3
0.4
0.5
a
0.16
0.14
0.12
0.10
0.08
0.06
0.04
0.02
0.00
Ψ_b(p)
0
1
2
3
4
5
p
a/a_0=0.1
a/a_0=0.5

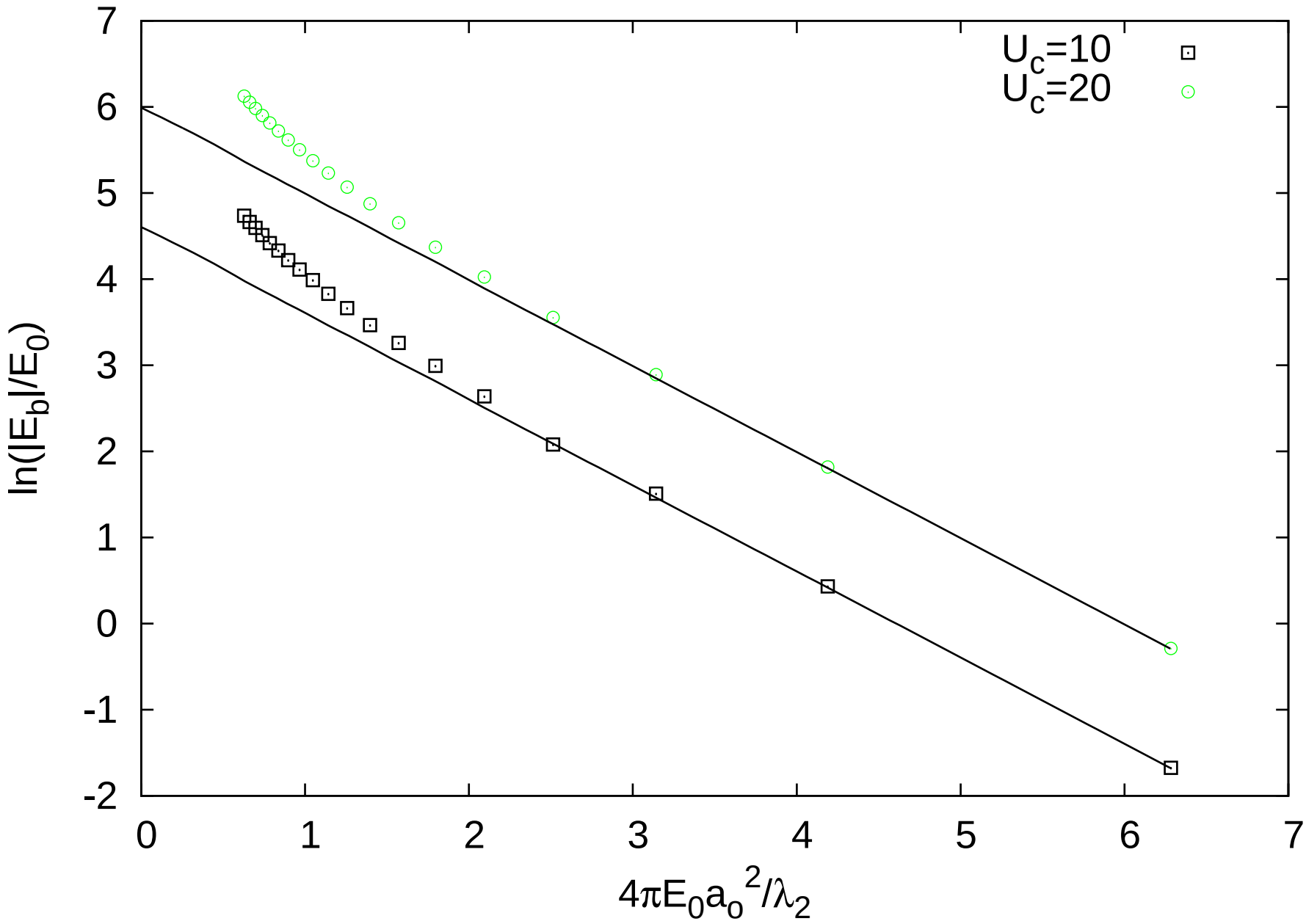
U_c=10
U_c=20
$\ln(|E_b|/E_0)$
$4\pi E_0 a_o^2/\lambda_2$
7
6
5
4
3
2
1
0
-1
-2
0
1
2
3
4
5
6
7